Published in final edited form as:

FASEB J. 2022 November ; 36(11): e22579. doi:10.1096/fj.202201114R.

Resolution of inflammation via RvD1/FPR2 signaling mitigates Nox2 activation and ferroptosis of macrophages in experimental abdominal aortic aneurysms

Amanda C. Filiberto,
Zachary Ladd,
Victoria Leroy,
Gang Su,
Craig T. Elder,
Eric Y. Pruitt,
Sara E. Hensley,
Guanyi Lu,
Joseph B. Hartman,
Ali Zarrinpar,
Ashish K. Sharma,
Gilbert R. Upchurch Jr

Department of Surgery, University of Florida, Gainesville, Florida, USA

Abstract

Abdominal aortic aneurysm (AAA) formation is characterized by inflammation, leukocyte infiltration, and vascular remodeling. Resolvin D1 (RvD1) is derived from ω-3 polyunsaturated fatty acids and is involved in the resolution phase of chronic inflammatory diseases. The aim of this study was to decipher the protective role of RvD1 via formyl peptide receptor 2 (FPR2) receptor signaling in attenuating abdominal aortic aneurysms (AAA). The elastase-treatment model of AAA in C57BL/6 (WT) mice and human AAA tissue was used to confirm our hypotheses. Elastase-treated $FPR2^{-/-}$ mice had a significant increase in aortic diameter, proinflammatory cytokine production, immune cell infiltration (macrophages and neutrophils), elastic fiber disruption, and decrease in smooth muscle cell α-actin expression compared to

Correspondence Gilbert R. Upchurch Jr., Department of Surgery, University of Florida, PO Box 100286, Gainesville, FL 32610, USA. gib.upchurch@surgery.ufl.edu.
Amanda C. Filiberto and Zachary Ladd contributed equally to this study.

AUTHOR CONTRIBUTIONS

Ashish K. Sharma and Gilbert R. Upchurch Jr. designed the research; Amanda C. Filiberto, Zachary Ladd, Victoria Leroy, Gang Su, Craig T. Elder, Eric Y. Pruitt, Sara E. Hensley, Guanyi Lu, Joseph B. Hartman, and Ashish K. Sharma performed the research; Ali Zarrinpar provided human aortic tissue; Ashish K. Sharma, and Gilbert R. Upchurch Jr. analyzed the data; Amanda C. Filiberto, Ashish K. Sharma, and Gilbert R. Upchurch Jr. wrote the manuscript with contributions from all authors; and all authors reviewed and approved the final manuscript.

SUPPORTING INFORMATION

Additional supporting information can be found online in the Supporting Information section at the end of this article.

DISCLOSURES

The authors have no conflict of interest in connection with this article.

elastase-treated WT mice. RvD1 treatment attenuated AAA formation, aortic inflammation, and vascular remodeling in WT mice, but not in FPR2$^{-/-}$ mice. Importantly, human AAA tissue demonstrated significantly decreased FPR2 mRNA expression compared to non-aneurysm human aortas. Mechanistically, RvD1/FPR2 signaling mitigated p47^{phox} phosphorylation and prevented hallmarks of ferroptosis, such as lipid peroxidation and Nrf2 translocation, thereby attenuating HMGB1 secretion. Collectively, this study demonstrates RvD1-mediated immunomodulation of FPR2 signaling on macrophages to mitigate ferroptosis and HMGB1 release, leading to resolution of aortic inflammation and remodeling during AAA pathogenesis.

Keywords

abdominal aortic aneurysms; ferroptosis; formyl peptide receptor 2; HMGB1; macrophages; resolvin D1

1 | INTRODUCTION

The pathophysiology of abdominal aortic aneurysm (AAA) remains elusive, but likely involves vascular inflammation characterized by leukocyte infiltration of the aortic wall associated with the production of proinflammatory cytokines.[1] The resolution of inflammation is now recognized as an active process mediated by specialized pro-resolving lipid mediators (SPMs) and dysregulation of inflammation resolution can significantly contribute to chronic inflammatory diseases.[2-4] SPMs include several structurally different families, including lipoxins from arachidonic acid, resolvins of the D- and E-series, protectins, and maresins, which are derived from the omega-3 fatty acids eicosapentaenoic acid and docosahexanoic acid (DHA).[5] The role of SPMs in the resolution of inflammation in AAAs has yet to be fully elucidated, as the unique properties of these bioactive lipid derivatives are postulated to modulate inflammation-resolution signaling pathways, thereby demonstrating a clinically applicable therapeutic strategy for the treatment of chronic vascular diseases.[2]

RvD1 (7S,8R,17S-trihydroxy-4Z,9E,11E,13Z,15E,19Z-docosahexaenoic acid) is a metabolite of docosahexaenoic acid (DHA) that modulates the resolution phase of the inflammatory response.[6,7] These immunomodulatory functions are mediated by FPR2, a type of G-protein-coupled receptors (GPCRs).[8-10] FPRs are a diverse family of seven transmembrane chemoattractant GPCRs that are classified as pattern recognition receptors located on immune cells and have the unique ability to recognize both pathogen-associated and damage-associated molecular patterns (PAMPs and DAMPs).[11] FPR2 can bind to various peptides and ligands, including RvD1, Lipoxin A4, human peptide humanin, and chemokine variant sCKb8-1, to convey contrasting biological signals.[12,13] We have previously described that exogenous treatment with RvD1 inhibits aortic dilation via mitigation of neutrophil extracellular traps (NET) formation during AAA.[14] However, the complexities of mechanistic signaling relative to ligand–receptor-mediated interactions associated with RvD1-mediated attenuation of aortic inflammation and cell death pathways remain unknown in aneurysmal pathology.

One of the characteristics of AAA formation and rupture is programmed cell death that involves progressive smooth muscle cell loss, as well as endothelial cell injury and death leading to aortic degeneration.[15] While apoptosis and NETosis have been shown to mediate AAA formation, other types of cell death have also been recently characterized in cardiovascular pathologies, that is, necroptosis, pyroptosis, and autophagy. In particular, the role of ferroptosis which is an iron-dependent cell death, and characterized by accumulation of lipid peroxides and redox disequilibrium, remains to be deciphered in the pathophysiology of AAA. Excessive iron accumulation in the aneurysm wall from luminal thrombus triggers lipid peroxidation and ROS generation leading to ferroptosis, aortic degeneration, and subsequent rupture.[16-18] Ferroptosis has been recently described to involve lipid peroxidation and release of danger-associated molecular pattern molecule, HMGB1.[19] We have previously described the putative role of macrophage-dependent HMGB1 via a NADPH oxidase (Nox2)-dependent pathway in AAA formation.[20] However, the role of ferroptosis in macrophage activation and HMGB1 release has not been fully evaluated from the perspective of AAA formation.

Therefore, the objective of this study was to determine if RvD1-mediated protection against AAA formation involves FPR2-dependent signaling, and to decipher the mechanistic pathways involved in macrophage activation during this process. Using a topical elastase-treatment murine model, we investigated if RvD1-mediated protection from AAAs is regulated via FPR2 on macrophages leads to attenuation of inflammation, immune cell activation, and proinflammatory cytokine production, as well as maintenance of smooth muscle cell integrity. The RvD1/FPR2 signaling on macrophages was mechanistically deciphered by Nox2 activation, ferroptosis, and HMGB1 release to delineate the contributory role of this inflammation-resolution pathway in modulating aortic inflammation and vascular remodeling during AAA formation.

2 | MATERIALS AND METHODS

2.1 | Human aortic tissue analysis

Collection of human aortic tissue was approved by the University of Florida Institutional Review Board (#IRB201902782). Consent was obtained from all patients before surgery. Aortic tissue from male patients was resected during open surgical AAA repair, as well as during organ transplant donor operations (controls). Tissue was homogenized in Trizol, and RNA was purified per manufacturer's protocol (Qiagen, Valencia, CA).

2.2 | Animals

Adult male 8–12-week-old C57BL/6 (wild-type; WT) and FPR2$^{-/-}$ mice were obtained from Jackson Laboratory (Bar Harbor, ME, USA) and Idorsia Pharmaceuticals, Switzerland, respectively. Mice were maintained in a temperature-controlled room (25°C) on a 12-h light/dark cycle with free access to food and water. All animal experimentation was approved by the University of Florida Institutional Animal Care and Use Committee (protocol # 201910902).

2.3 | Murine elastase model of aneurysm formation

AAA formation was induced using a topical elastase model, as previously described.[21] Porcine pancreatic elastase (5 μl; Sigma-Aldrich, St. Louis, MO, 7 units/mg protein) or heat-inactivated elastase (at 90°C for 30 min) as a control was applied topically to the exposed aortic adventitia for 5 min. Aortas were collected on days 3, 7, or 14 after elastase application. Aortic diameters were determined by video micrometry using Leica Application Suite 4.3 software (Leica Microsystems). The aortas were collected and stored at −80°F or incubated overnight in paraformaldehyde solution for histology. Iron concentration in aortic tissue extracts was measured using an iron assay kit, per the manufacturer's instructions (Millipore Sigma, St. Louis, MO).

2.4 | FPR2 expression quantification

RNA was isolated from human aortic tissue from AAA patients and control subjects using Total Exosome RNA and Protein Isolation Kit (Thermo Fisher Scientific). cDNA was synthesized using the iScript cDNA Synthesis Kit (BioRad, Hercules, CA). Quantitative (real-time) RT-PCR was performed with primer sets (MWG/Operon, Huntsville, AL) in conjunction with SsoFast EvaGreen Supermix (BioRad, Hercules, CA), as previously described.[22] To evaluate expression of FPR2 receptor in human aortic tissue, the following primers were used: FPR2 Fwd: GGCTACACTGTTCTGCGGAT, FPR2 Rev: CACCCAGATCACAAGCCCAT, GAPDH Fwd: TTGATGGCAACAATCTCCAC, GAPDH Rev: CGTCCCGTAGACAAAATGGT. Gene expression was calculated by using the relative quantification method according to the following equation: $2(-\Delta CT)$, where ΔCT = (average gene of interest) – (average reference gene), where GAPDH was used as the reference gene. Each PCR reaction was carried out in triplicate, and the relative quantification of gene expression was quantified as fold change.

2.5 | Cytokine multiplex assay

Cytokine content in murine aortic tissue homogenates and cell culture supernatants was quantified using the Bioplex Bead Array technique using a multiplex cytokine panel assay (Bio-Rad Laboratories, Hercules, CA) per the manufacturer's instructions. HMGB1 was measured in cell culture supernatants using an ELISA kit per the manufacturer's instructions (IBL International, Hamburg, Germany).

2.6 | Histology and Immunohistochemistry

Aortic tissue was fixed in 4% buffered formaldehyde overnight, transferred to 70% ethanol, and embedded in paraffin. Antibodies for immunohistochemical staining were anti-rat Mac-2 for macrophages (1:10000; Cedarlane Laboratories, Burlington, ON, Canada), anti-mouse neutrophils for polymorphonuclear neutrophils (PMNs) (1:10000; AbD Serotec, Oxford, United Kingdom), and anti-mouse α smooth muscle actin (α-SMA) for α-SMA (1:1000; Santa Cruz Biotechnology). Images were acquired with 20× magnification by an Olympus microscope equipped with a digital camera (Olympus America, Center Valley, PA, USA) and ImagePro software (Media Cybernetics, Rockville, MD, USA). For grading, the positive staining area of entire aortic tissue sample was selected and measured using integrated optical density of each section by independent observers blinded to study groups.

2.6.1 | Immunofluorescence staining—Harvested human aortic tissue was fixed in 10% buffered formalin overnight and embedded in paraffin. Immunofluorescence staining on aortic sections was performed to identify co-localization of CD68 and FPR2 expressions. Slides underwent deparaffinization using Xylene (Millipore Sigma, Burlington, MA) and were hydrated in a series of graded ethanol solutions. Sections underwent antigen retrieval via heat and citrate buffer (Vector Labs, Burlingame, CA). Tissue sections were blocked for 30 min with 2.5% normal Horse Serum (Vector Labs), and incubated with primary CD68 (1:500; Invitrogen, Waltham, MA) and FPR2 (1:50; Invitrogen) antibodies diluted in 1% BSA overnight at 4°C. Sections were washed with PBS containing 0.01% tween and incubated with donkey α-mouse Alexa Fluor 488 (1:200; Invitrogen) and donkey α-rabbit Alexa Fluor 647 (1:200; Invitrogen) secondary antibodies diluted in 1% BSA for 1 h at room temperature. Autofluorescence was quenched with Vector® TrueVIEW® Autofluorescence Quenching Kit (Vector Labs) per manufacturer's instructions. Sections were mounted with VECTASHIELD Vibrance® Antifade Mounting Medium containing DAPI for nuclear staining (Vector Labs). Triple staining was visualized using a Zeiss LSM 710 confocal microscope (Zeiss Group, Oberkochen, Germany) and captured at 63× magnification.

2.6.2 | In vitro experiments—Primary F4/80+ macrophages were purified from WT or FPR2$^{-/-}$ mice spleens per the manufacturer's protocol (Miltenyi Biotec, Germany). Primary aortic smooth muscle cells (SMCs) were purified from C57BL/6 mice as previously described.[23] Macrophages were exposed to transient elastase treatment for 5 min followed by washing the cells with PBS and replacing the media with/without RvD1 (100 nM). For evaluation of reactive oxygen species (ROS), cells were incubated with 10 μM dichlorofluorescein (DCF dye; Molecular Probes, Grand Island, NY) for 5 min and washed with PBS and analyzed 6 h later. Quantification of DCF dye in macrophages was performed using an OxiSelect Intracellular ROS assay kit as instructed (Cell Biolabs, San Diego, CA). All DCF solutions were protected from light to prevent light-induced auto-oxidation. Lipid peroxidation (MDA; Millipore Sigma, St. Louis, MO) and glutathione (GSH; Cayman Chemicals, Ann Arbor, MI) were measured in cell culture or tissue extracts using colorimetric assay kits, per the manufacturer's instructions. Separate macrophage cultures were also treated with erastin (10 μM; ferroptosis activator; Cayman Chemicals, Minneapolis, MN) with/without ferrostatin-1 (0.5 μM; selective inhibitor of ferroptosis; Cayman Chemicals) and analyzed for MDA and GSH expressions in macrophage culture extracts after 6 h. Nrf2 transcription factor activation in nuclear extracts was measured using a colorimetric assay kit (Abcam, Cambridge, UK). Separate experiments were also performed for conditioned media transfer (CMT) using macrophages and SMCs. Macrophages from WT or FPR2$^{-/-}$ mice were grown to confluency in 6-well plates and exposed to transient elastase treatment with/without RvD1 treatment. After 6 h, CMT was performed to SMC cultures and MMP2 activity was measured after 24 h (Luminex bead array, Millipore Sigma).

2.6.3 | NADPH oxidase activity—NADPH oxidase activity was measured by chemiluminescence in macrophage cell cultures using a Lumimax Superoxide Anion

Detection Kit (Agilent Technologies, Santa Clara, CA), as per the manufacturer's instructions.

2.6.4 | p47^{phox} phosphorylation—A colorimetric cell-based ELISA was used to measure p47^{phox} protein phosphorylation (Assay Biotechnology, Sunnyvale, CA). Primary murine F4/80+ macrophages (2×10^4/well) were plated, and the expression profile of phosphorylated versus total p47^{phox} was measured under various conditions. The absorbance values obtained for phosphorylated p47^{phox} were normalized to the absorbance values for total p47^{phox} as well as for GAPDH, per the manufacturer's instructions.

2.6.5 | Statistical analysis—Values are means ± standard error of mean (SEM), and statistical evaluation was performed with Prism 6 software (GraphPad, La Jolla, CA, USA). A Student's *t* test with nonparametric Mann–Whitney or Wilcoxon test was used for pair-wise comparisons of groups. One-way analysis of variance (ANOVA) after post-hoc Tukey's test was used to determine the differences among multiple comparative groups. A value of $p < .05$ was considered statistically significant.

3 | RESULTS

3.1 | AAA formation is exacerbated by deletion of FPR2 receptors

Using the topical elastase model, WT and FPR2$^{-/-}$ mice were treated with either elastase or heat-inactivated elastase on day 0 and harvested on day 14 (Figure 1A). Elastase-treated WT mice had significantly increased aortic diameter compared to controls (127.4% ± 8.4% vs. 1.4% ± 0.5%; $p < .0001$, Figure 1B,C). Importantly, elastase-treated FPR2$^{-/-}$ mice had a significant increase in aortic diameter compared to elastase-treated WT mice (165.4% ± 16.3% vs. 127.4% ± 8.4%; $p = .03$, Figure 1B,C). As an important clinical correlation, aortic tissue from human AAA patients demonstrated significantly decreased FPR2 mRNA expression compared to controls (Figure S1). Additionally, the co-expression of FPR2 receptors on human macrophages was also markedly decreased in human AAA tissue compared to controls (Figure S2).

3.2 | Aortic inflammation and remodeling are regulated via FPR2-dependent signaling

Elastase-treated FPR2$^{-/-}$ mice also demonstrated a marked increase in immune cell infiltration and disrupted aortic morphology as seen by comparative histology and immunostaining of aortic tissue, which revealed a significant increase in inflammatory cell (macrophages and neutrophils) infiltration, and elastic fiber disruption, as well as a decrease in smooth muscle α-actin expression compared to elastase-treated WT mice (Figure 2). Elastase-treated FPR2$^{-/-}$ mice also had a significant increase in cytokine production (IFN-γ, IL-1β, IL-17, MIP-2, MCP-1, TNF-α, and HMGB1) and MMP2 expression, compared to elastase-treated WT mice (Figure 3). There were no significant differences observed for IL-6 and IL-10 expression between elastase-treated WT and FPR2$^{-/-}$ mice. Taken together, these results demonstrate that deletion of FPR2 exacerbates aortic inflammation and vascular remodeling during AAA formation in the murine elastase AAA model.

3.3 | RvD1-mediated protection against AAA formation is mediated via an FPR2-dependent mechanism

Mice were treated with either elastase or heat-inactivated elastase on day 0 and injected with vehicle or RvD1 (4 ng/g body weight) on postoperative days 1 through 13 and harvested on day 14 (Figure 4A). RvD1 administration attenuated AAA formation in elastase-treated WT mice compared to untreated mice (62.9% ± 8.3% vs. 134% ± 8.1%; $p = .0004$). However, RvD1 administration did not mitigate AAA formation in elastase-treated FPR2$^{-/-}$ mice compared to untreated elastase-exposed FPR2$^{-/-}$ mice (143.7% ± 9.5% vs. 175.4% ± 14.9%; $p = .15$; Figure 4B,C). Immunohistology analyses demonstrated a marked decrease in neutrophil and macrophage infiltration, and elastin fiber disruption as well as increase in SM α-actin expression in RvD1-treated WT mice compared to RvD1-treated FPR2$^{-/-}$ mice (Figure 5). A significant attenuation of proinflammatory cytokine expression (IFN-γ, IL-1β, IL-17, MIP-2, MCP-1, TNF-α, IL-6, and HMGB1), and MMP2 expression as well as an increase in anti-inflammatory IL-10 expression in aortic tissue was observed in RvD1-treated WT mice compared to untreated mice (237 ± 25 vs. 63.1 ± 15.5 pg/ml; $p < .0001$; Figure 6). However, RvD1 administration in elastase-exposed FPR2$^{-/-}$ mice did not mitigate proinflammatory cytokine expression and MMP2 expression, or upregulate IL-10 expression, compared to untreated elastase-exposed FPR2$^{-/-}$ mice.

3.4 | RvD1/FPR2 signaling attenuates ferroptosis in AAA tissue

To investigate the mechanistic signaling of RvD1-mediated protection in murine AAAs, we focused on the excessive iron-mediated cell death (ferroptosis) pathway. Therefore, we analyzed the expression of key ferroptosis markers, that is, iron content, malondialdehyde (MDA), and glutathione (GSH) levels in murine aortic tissue from the experimental elastase-treatment model. The measurement of total iron content and Fe^{2+} in elastase-treated WT mice was significantly elevated at day 14 (Figure 7A). Moreover, the expression of lipid peroxidation product (MDA), a mediator of ferroptosis, was significantly increased in elastase-treated WT mouse AAA tissue at days 3, 7, and 14 compared to respective heat-inactivated elastase controls (Figure 7B). Also, depletion of glutathione (GSH) levels was observed in elastase-treated WT mice on days 3, 7, and 14 compared to controls (Figure 7C). Next, we delineated the effect of RvD1/FPR2 signaling on the signaling mediators of ferroptosis during AAA formation. Treatment with RvD1 significantly mitigated MDA expression and increased GSH levels in aortic tissue from elastase-treated WT mice, but not in elastase-treated FPR2$^{-/-}$ mice, compared to untreated controls on day 14 (Figure 7D,E). These results demonstrate that ferroptosis during murine AAA can be negatively modulated by RvD1 treatment via FPR2-dependent signaling.

3.5 | Nox2 inactivation by RvD1/FPR2 mitigates ferroptosis in macrophages

We previously demonstrated that Nox2 activation in macrophages upregulates danger-associated molecular pattern (DAMP) signaling to regulate aortic inflammation in AAA.[20] Also, we have shown that RvD1 treatment can modulate M2 macrophage polarization to decrease vascular inflammation.[14] Therefore, we investigated the correlation between RvD1-mediated protection in macrophages during AAA via FPR2-dependent signaling to modulate the NADPH oxidase subunit, $p47^{phox}$, in regulating oxidative stress, lipid peroxidation, and

ferroptosis. First, we measured superoxide anion production and reactive oxygen species (ROS) generation in F4/80+ macrophages from WT and FPR2$^{-/-}$ mice. A significant increase in superoxide anion and ROS was observed after transient elastase treatment of macrophages, which was significantly decreased by RvD1 treatment in WT mice, but not in FPR2$^{-/-}$ mice (Figure 8A,B). Furthermore, phosphorylation of p47^{phox} subunit, which leads to activation of NADPH oxidase (Nox2) complex, was significantly increased by elastase treatment of WT and FPR2$^{-/-}$ macrophages compared to respective controls (Figure 8C). However, RvD1 treatment mitigated p47^{phox} phosphorylation in elastase-treated macrophages from WT mice, but not in elastase-treated FPR2$^{-/-}$ macrophages. Moreover, RvD1 treatment attenuated MDA expression and increased GSH levels in cell culture extracts of elastase-exposed WT macrophages, but not in elastase-exposed FPR2$^{-/-}$ macrophages (Figure 8D). Separate cultures of macrophages from WT or FPR2$^{-/-}$ mice were treated with erastin (ferroptosis activator), ferrostatin-1 (ferroptosis inhibitor), or RvD1. A significant increase in MDA expression and decrease in GSH levels was observed in erastin-treated macrophage cultures which was inhibited by RvD1 treatment in macrophages from WT mice, but not in macrophages from FPR2$^{-/-}$ macrophages (Figure S3). We also measured the nuclear translocation of antioxidant transcription factor, Nrf2, which was significantly increased in elastase-treated macrophages compared to controls (Figure 8E). RvD1 treatment significantly decreased Nrf2 nuclear translocation, as well as HMGB1 release, in elastase-treated macrophages from WT mice, but not in FPR2$^{-/-}$ mice (Figure 8E-G). Finally, a multifold increase in HMGB1 expression was observed in erastin-treated macrophage cultures that was attenuated by RvD1 treatments in macrophages from WT mice, but not in macrophages from FPR2$^{-/-}$ macrophages (Figure S4). Collectively, these results demonstrate that RvD1/FRP2 signaling leads to blockade of p47^{phox} phosphorylation, which protects against lipid peroxidation, GSH depletion and Nrf2 translocation, all hallmarks of ferroptosis (Figure 8H).

Conditioned media transfer of elastase-exposed macrophages increased MMP2 activity by SMCs, which was mitigated by RvD1 treatment in WT macrophages, but not in FPR2$^{-/-}$ macrophages (Figure 8I,J). These results suggest that the crosstalk between macrophages and SMCs to mediate AAA formation is negatively modulated by RvD1/FPR2 mediated signaling, which prevents macrophage activation and HMGB1 release to attenuate aortic tissue inflammation and remodeling (Figure 8K).

4 | DISCUSSION

Dysregulation of inflammation resolution can initiate a cascade of events that leads to tissue damage and defective clearance of dead cell debris, leading to chronic inflammatory cardiovascular disorders.[24-26] To investigate the pathways involved in failure of inflammation resolution, this study characterized the role of specialized pro-resolving lipid mediator, RvD1, and the downstream signaling executed via the receptor, FPR2, in mitigating AAA formation. Our results demonstrated that RvD1 treatment can effectively decrease aortic inflammation, leukocyte transmigration, and vascular remodeling during AAA formation in a FPR2-dependent manner. Furthermore, we observed that the hallmarks of excessive iron-mediated cell death (ferroptosis) pathways, which are elevated in AAA formation, can be subdued by RvD1/FPR2-dependent signaling. Mechanistically, we further

defined that macrophage activation leads to aortic inflammation and triggers smooth muscle cell-dependent vascular remodeling, which can be mitigated by RvD1/FPR2 signaling via inactivation of Nox2 and ferroptosis-related signaling pathways. Collectively, these results demonstrate the ability of RvD1/FPR2 to prevent ferroptosis-induced macrophage activation, thereby promoting the resolution of inflammation during AAA formation.

Protective actions of SPMs have been demonstrated in numerous models of inflammation, including atherosclerosis, diabetes, peritonitis, colitis, and airway inflammation, but remain to be elucidated in the pathogenesis of AAA.[27] AAA is a morbid vascular condition characterized by inflammation of the aortic wall, elevated protease activity and impaired resolution. Infiltration of lymphocytes and macrophages into the aortic wall promotes a matrix degradation, and SPMs have been shown to play a role in attenuation of aortic inflammation through alterations in matrix metabolism.[14,28,29] We have previously demonstrated the ability of Resolvin D2 to influence macrophage polarization toward an anti-inflammatory M2 profile resulting in decreased aneurysm size via modulation of matrix metalloproteinases and inflammatory cytokines.[14] Also, we have shown that RvD1 can inhibit neutrophil extracellular trap (NETosis) formation to decrease AAA formation.[30] However, the ligand–receptor interaction, especially with RvD1 binding of specific receptor FPR2, on immune cells like macrophages and mechanistic pathways involved in resolution of inflammation remain to be delineated in AAA formation.

FPR2 can promote either proinflammatory or pro-resolving signaling, that is dependent on the ligand, which triggers downstream signaling pathways.[4,7] Previous studies have shown that interaction of ALX/FPR2 receptor by LxA_4 or RvD1 can promote pro-reparative phenotype and increases efferocytosis.[31] The pro-resolving profile can be mediated by annexin A1 and lipoxin A4, which initiates macrophage efferocytosis, whereas LL-37 peptide and serum amyloid protein A modulates leukocyte activation and recruitment for a proinflammatory action.[32-34] Our results and a previous report has shown that the human aortic tissue displays downregulation of FPR2 expression in AAA, thereby showing the relevance of dysregulation of resolution pathways in a chronic inflammatory state.[35] These findings underscore the importance of using exogenous pro-resolving mediators to target the anti-inflammatory potential of FPR2 to circumvent the ratio of pro- versus anti-inflammatory signaling mediators. The interaction of RvD1/FPR2 has been shown to play a role in the resolution of inflammation through the recruitment of monocytes and apoptosis of neutrophils, regulation of neutrophil migration, and promotion of tissue repair.[36-38] Our results suggest that deletion of FPR2 prevents endogenous SPMs, like RvD1 and likely LxA4, to inherently control the resolution of aortic inflammation. Therefore, the $FPR2^{-/-}$ mice display enhanced inflammation, vascular remodeling as well as increased aortic diameter. More importantly, the immunomodulation of FPR2 signaling by exogenous RvD1 identifies a novel mechanism in resolution of aortic inflammation and vascular remodeling during AAA pathogenesis.

Progressive SMC loss is a crucial feature of AAA pathogenesis that contributes to aortic dysfunction and degeneration, aortic dissection, and ultimately, rupture. A growing body of evidence supports a critical role for programmed cell death in the pathogenesis of AAA formation, and the relative inhibitors of various types of programmed cell death

represent a promising therapeutic strategy. Although the literature has defined programmed cell death, like apoptosis, in mediating SMC and endothelial cell loss, there are also other non-apoptotic cell death pathways like ferroptosis, necroptosis, pyroptosis, and NETosis that are now being increasingly implicated in aneurysm formation.[15] One of the hallmarks of AAA formation is a thrombus formation which involves increased accumulation of iron.[17,18] Ferroptosis is a programmed iron-dependent cell death, characterized by accumulation of lipid peroxides (LOOH) and redox disequilibrium. Iron overload causes excessive iron deposition in various cells resulting in nonreversible tissue damages and organ failure via oxidative damage characterized by mitochondrial changes due to excessive accumulation of iron-dependent lipid peroxidation products. The mechanisms of ferroptosis, that is, intracellular iron accumulation, depletion of glutathione, increase in lipid peroxidation and ROS formation, as well as Nrf2 nuclear translocation are closely related to many physiological processes, including iron metabolism, amino acids metabolism, and lipid metabolism.[39] Further exploration of ferroptosis indicator proteins such as SLC7A11 and GFX4, as well as the applicability of ferroptosis inhibitors such as ferrostatin-1 and liproxstatin-1, in aneurysm pathology remain to be elucidated.

It is known that the pro-oxidative effects of iron on lipoproteins lead to aortic endothelial and macrophage activation.[40,41] Since our recent study showed that Resolvins can increase M2 macrophage polarization, we focused on the mechanistic signaling of RvD1 on macrophages via the FPR2 pathway.[14] Our current data also corroborate the immune signatures of ferroptotic pathways in macrophages to induce DAMP signaling by upregulating HMGB1 secretion, which we have previously shown to critically mediate aortic inflammation and vascular remodeling during AAA formation.[20] Importantly, the suppression of Nox2-mediated ROS generation and prevention of ferroptotic pathways by RvD1-mediated protection modulated HMGB1 release and downstream activation of SMCs. This cytoprotective activity of RvD1 could be attributable to cAMP production and PKA activation which appears to mediated by FPR2. A recent study has demonstrated that efferocytosis-induced ROS generation is associated with the activation of Nox2, the major NADPH oxidase complex present in macrophages.[42] The engulfment of apoptotic cells activates Nox2 in macrophages by inducing the association between the membrane-bound factor gp91^{phox} and cytosolic factor p47^{phox} on phagosomal membranes. Interestingly, it has been suggested that the macrophage phenotype, classified into proinflammatory M1 and anti-inflammatory M2, is controlled by cAMP, which can be modulated by RvD1/FPR2 signaling. Furthermore, recent studies have indicated that mechanisms of clearance of different modes of dead or dying cells via apoptosis or other modes of cell death, such as ferroptosis, can lead to efferocytosis and distinct physiological outcomes.[43,44] The process of efferocytosis specifically in aging diseases like AAA could be limited due to senescent cell-induced MerTK cleavage, a process that can be reversed by RvD1.[6,45] Therefore, it is conceivable that RvD1/FPR2 signaling on macrophages upregulates efferocytosis by inhibiting p47^{phox} phosphorylation and blocking ROS generation and ferroptosis. Future studies will be focused on delineating the RvD1-stimulated macrophages in preventing p47^{phox} phosphorylation to culminate in proteolysis of MerTK. Additionally, FPR1 and FPR2 receptor signaling on neutrophils has been shown to modulate chemotaxis and Nox2 activation causing oxidative stress and neutrophil activation in various diseases.[46,47] Our

previous study has shown that FPR1 receptors on activated neutrophils in AAA can be used as an SPECT imaging tool using a radiolabeled peptide, c-FLFLF.[48] Therefore, RvD1/FPR2 signaling on other pertinent immune cells like neutrophils, as well as resident cells such as aortic smooth muscle cells and endothelial cells, could also play a significant role in the pathogenesis of AAA and remains to be delineated. These findings will help our understanding of how innate pattern recognition receptor signaling links to proteolytic inactivation of MerTK thereby affecting efferocytosis efficiency of immune and resident cells and inflammation resolution in AAA.

A few limitations of our study exist for a translational strategy. First, although the topical elastase model provides an excellent experimental tool to investigate the early inflammatory signaling pathways in the vasculature and aortic wall during AAA, as it represents the hallmarks of human aneurysmal pathology such as macrophage infiltration, matrix degradation, increased MMP activation, elastin fiber degradation, and loss of smooth muscle integrity, but it lacks the chronicity and aortic rupture observed in clinical scenario.[49] Thus, these findings will be further delineated in our recently described chronic aortic aneurysm and rupture models.[50,51] Second, an effective strategy to mitigate chronic aortic inflammation and vascular remodeling will likely involve a combined therapeutic strategy using additional bioactive isoforms of SPMs such as MaR1, in combination with RvD1, for a synergistic and multifaceted approach to mitigate this vascular pathology.[52] The mechanistic approach of MaR1-dependent upregulation of SMC efferocytosis in combination with RvD1-mediated decrease in ferroptosis will be further deciphered in our large animal preclinical porcine AAA model.[53]

Taken together, our findings suggest that the pro-resolving lipid mediator RvD1 plays a pivotal role in the inactivation of macrophage-dependent ferroptosis and HMGB1 release to mitigate SMC-regulated vascular remodeling and AAA formation. RvD1-mediated protection is attributable to FPR2-dependent signaling on macrophages through inhibition of assembly of the Nox2 complex via prevention of $p47^{phox}$ phosphorylation. RvD1/FPR2 signaling also potently reversed ferroptosis-triggered signaling, and stimulated the antioxidant pathway via Nox2, thereby assisting in prevention of active and passive release of HMGB1 to mitigate downstream tissue inflammation and remodeling of the aortic tissue. These results suggest a novel mechanism that can be harnessed to alter the inflammation-resolution dysregulation, via the use of bioactive SPMs and synthetic derivatives, as targeted therapies for management of chronic inflammatory vascular diseases.

Supplementary Material

Refer to Web version on PubMed Central for supplementary material.

ACKNOWLEDGMENTS

This work was supported by the American College of Surgeons Resident Research Scholarship (ACF), R01HL153341 and R01HL138931 (GRU and AKS). We thank Dr. Ganesh Halade, University of South Florida, Tampa, and Idorsia Pharmaceuticals, Switzerland for providing the $FPR2^{-/-}$ mice for this study.

Funding information

American College of Surgeons (ACS); HHS | NIH | National Heart, Lung, and Blood Institute (NHLBI), Grant/Award Number: HL153341 and HL138931

DATA AVAILABILITY STATEMENT

The data that support the findings of this study are available in the Materials and Methods section as well as in the Supplementary Material of this article.

Abbreviations:

AAA	abdominal aortic aneurysm
FPR2	formyl peptide receptor
HMGB1	high mobility group box 1
MDA	malondialdehyde
Nrf2	nuclear factor erythroid factor 2-related factor 2
RvD1	resolvin D1
SPMs	specialized pro-resolving lipid mediators
α-SMA	alpha-smooth muscle cell actin

REFERENCES

1. Kuivaniemi H, Ryer EJ, Elmore JR, Tromp G. Understanding the pathogenesis of abdominal aortic aneurysms. Expert Rev Cardiovasc Ther. 2015;13:975–987. [PubMed: 26308600]
2. Serhan CN. Novel pro-resolving lipid mediators in inflammation are leads for resolution physiology. Nature. 2014;510:92–101. [PubMed: 24899309]
3. Basil MC, Levy BD. Specialized pro-resolving mediators: endogenous regulators of infection and inflammation. Nat Rev Immunol. 2016;16:51–67. [PubMed: 26688348]
4. Spite M, Claria J, Serhan CN. Resolvins, specialized proresolving lipid mediators, and their potential roles in metabolic diseases. Cell Metab. 2014;19:21–36. [PubMed: 24239568]
5. Serhan CN. Novel lipid mediators and resolution mechanisms in acute inflammation: to resolve or not? Am J Pathol. 2010;177:1576–1591. [PubMed: 20813960]
6. Gerlach BD, Marinello M, Heinz J, et al. Resolvin D1 promotes the targeting and clearance of necroptotic cells. Cell Death Differ. 2020;27:525–539. [PubMed: 31222041]
7. Krishnamoorthy S, Recchiuti A, Chiang N, Fredman G, Serhan CN. Resolvin D1 receptor stereoselectivity and regulation of inflammation and proresolving microRNAs. Am J Pathol. 2012;180:2018–2027. [PubMed: 22449948]
8. Krishnamoorthy S, Recchiuti A, Chiang N, et al. Resolvin D1 binds human phagocytes with evidence for proresolving receptors. Proc Natl Acad Sci U S A. 2010;107:1660–1665. [PubMed: 20080636]
9. Arnardottir H, Thul S, Pawelzik SC, et al. The resolvin D1 receptor GPR32 transduces inflammation resolution and athero-protection. J Clin Invest. 2021;131:e142883. [PubMed: 34699386]
10. Norling LV, Dalli J, Flower RJ, Serhan CN, Perretti M. Resolvin D1 limits polymorphonuclear leukocyte recruitment to inflammatory loci: receptor-dependent actions. Arterioscler Thromb Vasc Biol. 2012;32:1970–1978. [PubMed: 22499990]

11. Cooray SN, Gobbetti T, Montero-Melendez T, et al. Ligand-specific conformational change of the G-protein-coupled receptor ALX/FPR2 determines proresolving functional responses. Proc Natl Acad Sci U S A. 2013;110:18232–18237. [PubMed: 24108355]
12. Liu GJ, Tao T, Wang H, et al. Functions of resolvin D1-ALX/FPR2 receptor interaction in the hemoglobin-induced microglial inflammatory response and neuronal injury. J Neuroinflammation. 2020;17:239. [PubMed: 32795323]
13. Ramon S, Bancos S, Serhan CN, Phipps RP. Lipoxin A(4) modulates adaptive immunity by decreasing memory B-cell responses via an ALX/FPR2-dependent mechanism. Eur J Immunol. 2014;44:357–369. [PubMed: 24166736]
14. Pope NH, Salmon M, Davis JP, et al. D-series resolvins inhibit murine abdominal aortic aneurysm formation and increase M2 macrophage polarization. FASEB J. 2016;30:4192–4201. [PubMed: 27619672]
15. Chakraborty A, Li Y, Zhang C, Li Y, LeMaire SA, Shen YH. Programmed cell death in aortic aneurysm and dissection: a potential therapeutic target. J Mol Cell Cardiol. 2022;163:67–80. [PubMed: 34597613]
16. Honkanen P, Frosen JK, Abo-Ramadan U, Hernesniemi JA, Niemela MR. Visualization of luminal thrombosis and mural iron accumulation in giant aneurysms with ex vivo 4.7T magnetic resonance imaging. Surg Neurol Int. 2014;5:74. [PubMed: 24949217]
17. Piechota-Polanczyk A, Jozkowicz A, Nowak W, et al. The abdominal aortic aneurysm and intraluminal thrombus: current concepts of development and treatment. Front Cardiovasc Med. 2015;2:19. [PubMed: 26664891]
18. Sawada H, Hao H, Naito Y, et al. Aortic iron overload with oxidative stress and inflammation in human and murine abdominal aortic aneurysm. Arterioscler Thromb Vasc Biol. 2015;35:1507–1514. [PubMed: 25882069]
19. Wiernicki B, Maschalidi S, Pinney J, et al. Cancer cells dying from ferroptosis impede dendritic cell-mediated anti-tumor immunity. Nat Commun. 2022;13:3676. [PubMed: 35760796]
20. Sharma AK, Salmon MD, Lu G, et al. Mesenchymal stem cells attenuate NADPH oxidase-dependent high mobility group Box 1 production and inhibit abdominal aortic aneurysms. Arterioscler Thromb Vasc Biol. 2016;36:908–918. [PubMed: 26988591]
21. Laser A, Lu G, Ghosh A, et al. Differential gender- and species-specific formation of aneurysms using a novel method of inducing abdominal aortic aneurysms. J Surg Res. 2012;178:1038–1045. [PubMed: 22651981]
22. Sharma AK, Lu G, Jester A, et al. Experimental abdominal aortic aneurysm formation is mediated by IL-17 and attenuated by mesenchymal stem cell treatment. Circulation. 2012;126:S38–S45. [PubMed: 22965992]
23. Colonnello JS, Hance KA, Shames ML, et al. Transient exposure to elastase induces mouse aortic wall smooth muscle cell production of MCP-1 and RANTES during development of experimental aortic aneurysm. J Vasc Surg. 2003;38:138–146. [PubMed: 12844103]
24. Maskrey BH, Megson IL, Whitfield PD, Rossi AG. Mechanisms of resolution of inflammation: a focus on cardiovascular disease. Arterioscler Thromb Vasc Biol. 2011;31:1001–1006. [PubMed: 21508346]
25. Fredman G. Can inflammation-resolution provide clues to treat patients according to their plaque phenotype? Front Pharmacol. 2019;10:205. [PubMed: 30899222]
26. Halade GV, Lee DH. Inflammation and resolution signaling in cardiac repair and heart failure. EBioMedicine. 2022;79:103992. [PubMed: 35405389]
27. Conte MS, Desai TA, Wu B, Schaller M, Werlin E. Pro-resolving lipid mediators in vascular disease. J Clin Invest. 2018;128:3727–3735. [PubMed: 30168805]
28. Meital LT, Sandow SL, Calder PC, Russell FD. Abdominal aortic aneurysm and omega-3 polyunsaturated fatty acids: mechanisms, animal models, and potential treatment. Prostaglandins Leukot Essent Fatty Acids. 2017;118:1–9. [PubMed: 28288701]
29. Wales KM, Kavazos K, Nataatmadja M, Brooks PR, Williams C, Russell FD. N-3 PUFAs protect against aortic inflammation and oxidative stress in angiotensin II-infused apolipoprotein E−/− mice. PLoS One. 2014;9:e112816. [PubMed: 25398022]

30. Spinosa M, Su G, Salmon MD, et al. Resolvin D1 decreases abdominal aortic aneurysm formation by inhibiting NETosis in a mouse model. J Vasc Surg. 2018;68:93S–103S. [PubMed: 30470363]
31. Sun YP, Oh SF, Uddin J, et al. Resolvin D1 and its aspirin-triggered 17R epimer. Stereochemical assignments, anti-inflammatory properties, and enzymatic inactivation. J Biol Chem. 2007;282:9323–9334. [PubMed: 17244615]
32. Serhan CN, Chiang N, Van Dyke TE. Resolving inflammation: dual anti-inflammatory and pro-resolution lipid mediators. Nat Rev Immunol. 2008;8:349–361. [PubMed: 18437155]
33. Dufton N, Hannon R, Brancaleone V, et al. Anti-inflammatory role of the murine formyl-peptide receptor 2: ligand-specific effects on leukocyte responses and experimental inflammation. J Immunol. 2010;184:2611–2619. [PubMed: 20107188]
34. He R, Sang H, Ye RD. Serum amyloid A induces IL-8 secretion through a G protein-coupled receptor, FPRL1/LXA4R. Blood. 2003;101:1572–1581. [PubMed: 12393391]
35. Petri MH, Thul S, Andonova T, et al. Resolution of inflammation through the lipoxin and ALX/FPR2 receptor pathway protects against abdominal aortic aneurysms. JACC Basic Transl Sci. 2018;3:719–727. [PubMed: 30623131]
36. Ariel A, Serhan CN. Resolvins and protectins in the termination program of acute inflammation. Trends Immunol. 2007;28:176–183. [PubMed: 17337246]
37. Sekheri M, El Kebir D, Edner N, Filep JG. 15-Epi-LXA4 and 17-epi-RvD1 restore TLR9-mediated impaired neutrophil phagocytosis and accelerate resolution of lung inflammation. Proc Natl Acad Sci U S A. 2020;117:7971–7980. [PubMed: 32205444]
38. Serhan CN, Chiang N, Dalli J, Levy BD. Lipid mediators in the resolution of inflammation. Cold Spring Harb Perspect Biol. 2014;7:a016311. [PubMed: 25359497]
39. Zhang Y, Xin L, Xiang M, et al. The molecular mechanisms of ferroptosis and its role in cardiovascular disease. Biomed Pharmacother. 2022;145:112423. [PubMed: 34800783]
40. Vinchi F, Muckenthaler MU, Da Silva MC, Balla G, Balla J, Jeney V. Atherogenesis and iron: from epidemiology to cellular level. Front Pharmacol. 2014;5:94. [PubMed: 24847266]
41. Yang Y, Wang Y, Guo L, Gao W, Tang TL, Yan M. Interaction between macrophages and ferroptosis. Cell Death Dis. 2022;13:355. [PubMed: 35429990]
42. Lee HN, Surh YJ. Resolvin D1-mediated NOX2 inactivation rescues macrophages undertaking efferocytosis from oxidative stress-induced apoptosis. Biochem Pharmacol. 2013;86:759–769. [PubMed: 23856291]
43. Boada-Romero E, Martinez J, Heckmann BL, Green DR. The clearance of dead cells by efferocytosis. Nat Rev Mol Cell Biol. 2020;21:398–414. [PubMed: 32251387]
44. Maschalidi S, Mehrotra P, Keceli BN, et al. Targeting SLC7A11 improves efferocytosis by dendritic cells and wound healing in diabetes. Nature. 2022;606:776–784. [PubMed: 35614212]
45. Rymut N, Heinz J, Sadhu S, et al. Resolvin D1 promotes efferocytosis in aging by limiting senescent cell-induced MerTK cleavage. FASEB J. 2020;34:597–609. [PubMed: 31914705]
46. Liu M, Chen K, Yoshimura T, et al. Formylpeptide receptors are critical for rapid neutrophil mobilization in host defense against Listeria monocytogenes. Sci Rep. 2012;2:786. [PubMed: 23139859]
47. Martensson J, Sundqvist M, Manandhar A, et al. The two formyl peptide receptors differently regulate GPR84-mediated neutrophil NADPH oxidase activity. J Innate Immun. 2021;13:242–256. [PubMed: 33789297]
48. Shannon AH, Chordia MD, Spinosa MD, et al. Single-photon emission computed tomography imaging using formyl peptide receptor 1 ligand can diagnose aortic aneurysms in a mouse model. J Surg Res. 2020;251:239–247. [PubMed: 32172010]
49. Bhamidipati CM, Mehta GS, Lu G, et al. Development of a novel murine model of aortic aneurysms using peri-adventitial elastase. Surgery. 2012;152:238–246. [PubMed: 22828146]
50. Fashandi AZ, Hawkins RB, Salmon MD, et al. A novel reproducible model of aortic aneurysm rupture. Surgery. 2018;163:397–403. [PubMed: 29195736]
51. Lu G, Su G, Davis JP, et al. A novel chronic advanced stage abdominal aortic aneurysm murine model. J Vasc Surg. 2017;66:232–242.e4. [PubMed: 28274752]

52. Elder CT, Filiberto AC, Su G, et al. Maresin 1 activates LGR6 signaling to inhibit smooth muscle cell activation and attenuate murine abdominal aortic aneurysm formation. FASEB J. 2021;35:e21780. [PubMed: 34320253]

53. Cullen JM, Lu G, Shannon AH, et al. A novel swine model of abdominal aortic aneurysm. J Vasc Surg. 2019;70:252–260.e2. [PubMed: 30591288]

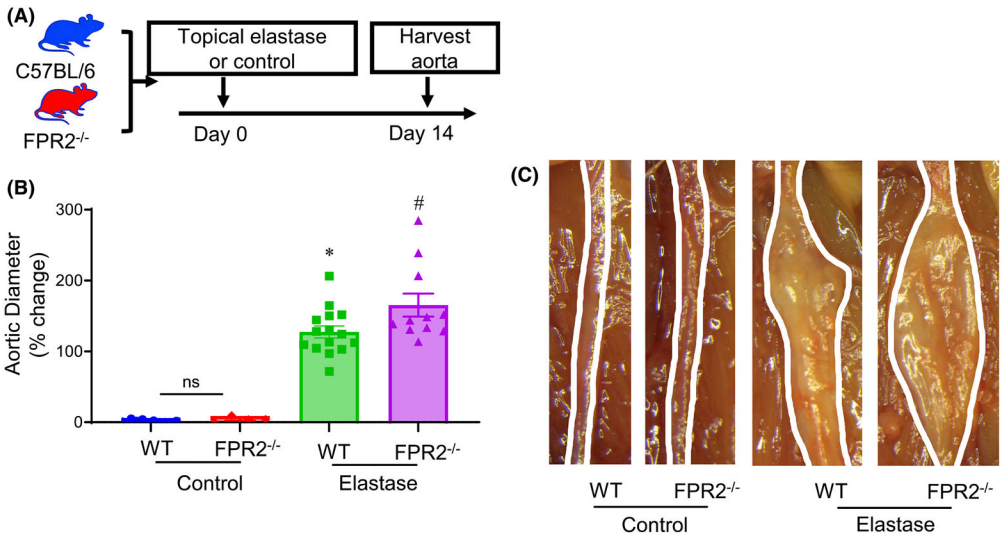

FIGURE 1.

FPR2 deletion exacerbates AAA formation. (A) Schematic description of the elastase-treatment model of AAA. WT and FPR2$^{-/-}$ mice were treated with elastase or deactivated elastase (heat -inactivated; controls) and aortic diameter was measured on day 14, and tissue was harvested for further analysis. (B) Elastase-treated FPR2$^{-/-}$ mice demonstrated a significant increase in aortic diameter compared with elastase-treated WT mice alone. (C) Representative images of aortic phenotype in all groups, ns, not significant. *$p < .0001$ versus. WT Control, $^{\#}p = .04$ versus. WT Elastase; ns, not significant; $n = 6–16$ mice/group.

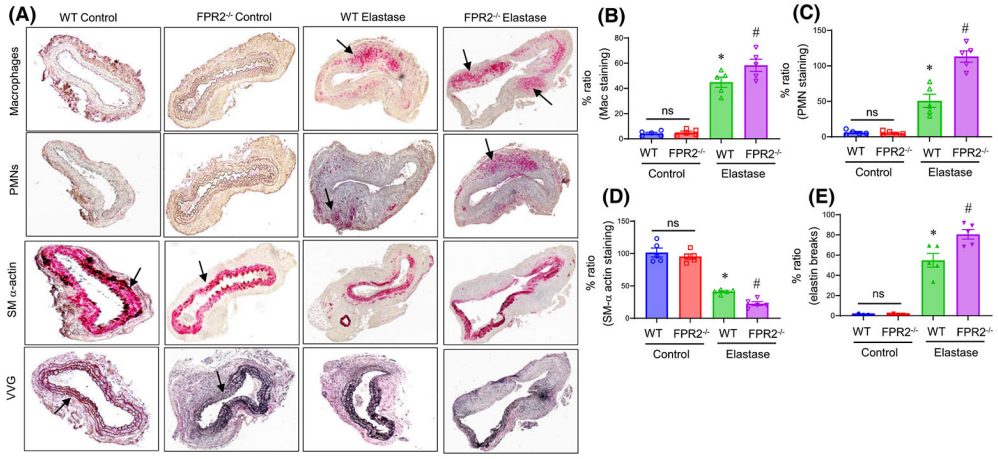

FIGURE 2.

(A) Comparative histology performed on day 14 indicates that elastase-treated FPR2$^{-/-}$ mice have a marked increase in neutrophil (PMN) and macrophage (Mac-2) infiltration, elastic fiber disruption (Verhoeff–Van Gieson staining for elastin) as well as a decrease in smooth muscle cell α-actin (SM α–actin) expression, compared to elastase-treated WT mice alone. (B–E) Quantification of immunohistochemical staining demonstrating a significant increase in macrophages and neutrophils (PMNs) and elastin degradation (VVG) staining, as well as decrease in smooth muscle α-actin expression in elastase-treated FPR2$^{-/-}$ aortic tissue compared with elastase-treated WT mice. No significant differences were observed between heat-inactivated elastase (control)-treated WT and FPR2$^{-/-}$ mice. Arrows indicate areas of immunostaining. *$p < .0001$ versus WT Control, $^{\#}p < .04$ versus WT Elastase; $n = 5$ mice/group.

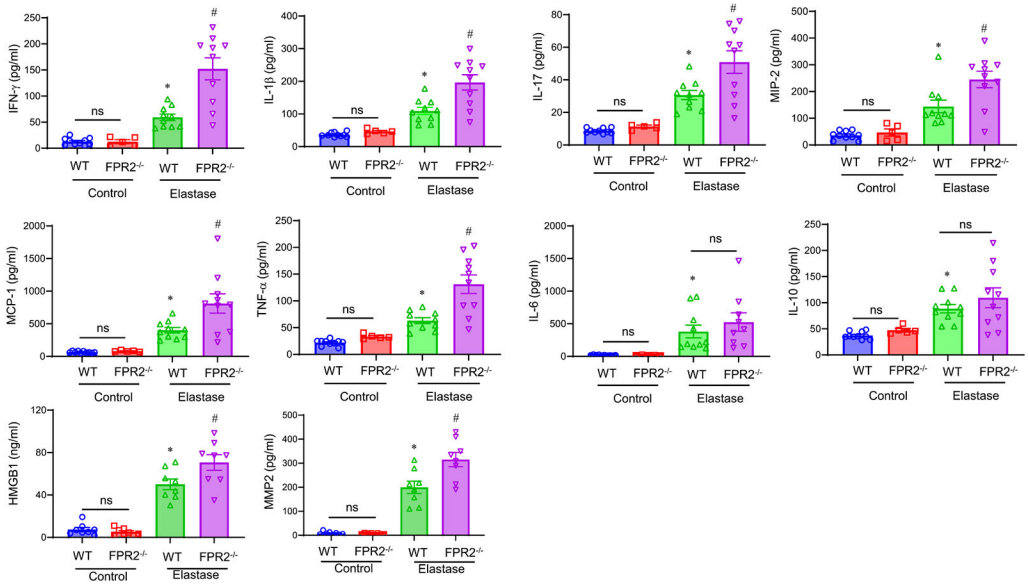

FIGURE 3.

Proinflammatory cytokine production is increased by FPR2 deletion. Aortic tissue from elastase-treated WT and FPR2$^{-/-}$ mice showed a significant exacerbation in proinflammatory cytokine/chemokine production and MMP2 expression compared to elastase-treated WT mice alone. There was no difference in the expression of anti-inflammatory cytokine, IL-10, between elastase-treated FPR2$^{-/-}$ mice compared to elastase-treated WT mice. *$p < .04$ versus WT Control; $^{\#}p < .01$ versus WT Elastase; ns, not significant; $n = 10$ mice/group.

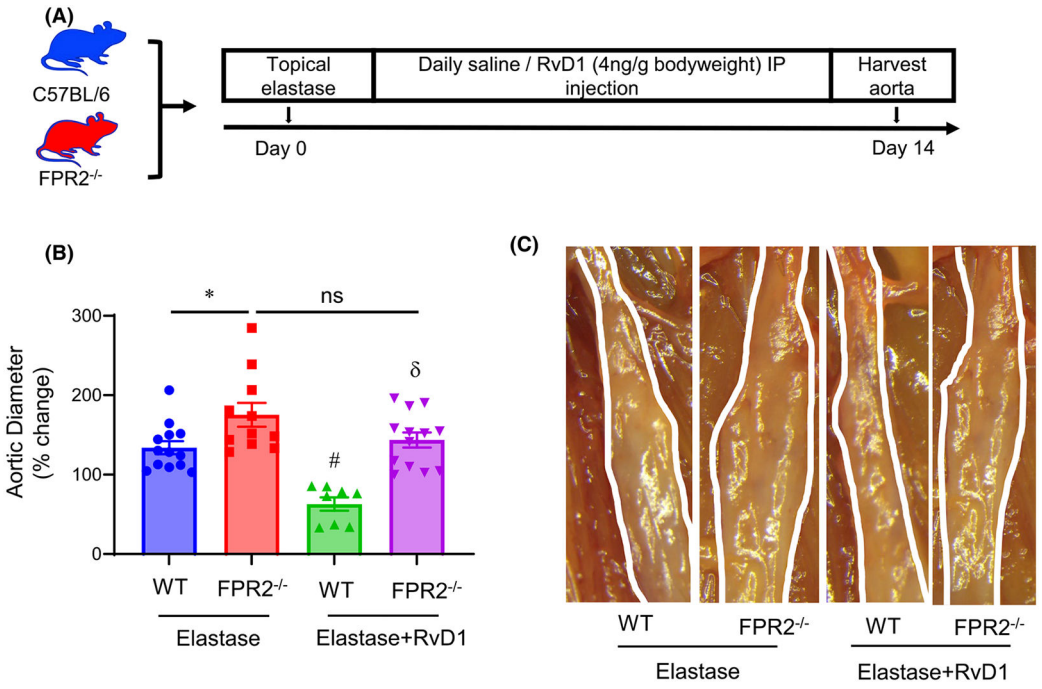

FIGURE 4.

RvD1-mediated attenuation of AAA formation is mediated via FPR2. (A) Schematic depicting the elastase-treatment model depicting the RvD1 treatment design. (B) RvD1-treated WT mice demonstrated significantly decreased aortic diameter compared with RvD1-treated FPR2$^{-/-}$ mice. (C) Representative images of aortic phenotype in all groups. *$p = .03$; $^{\#}p = .0004$ versus WT Elastase; $^{\delta}p < .0001$ versus WT Elastase+RvD1; ns, not significant; $n = 8–13$ mice/group.

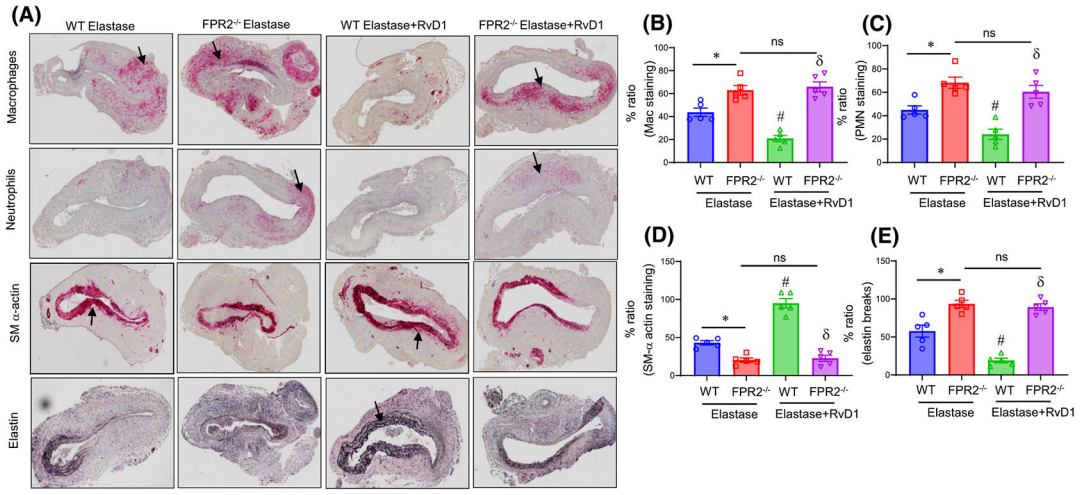

FIGURE 5.

(A) Comparative histology indicates that RvD1-mediated attenuation of immune cell infiltration, elastin fiber disruption and increased SM α-actin expression is blocked in RvD1-mediated FPR2$^{-/-}$ mice. (B–E) Quantification of immunohistochemical staining shows a significant decrease in polymorphonuclear neutrophil (PMNs) and macrophage (Mac-2) infiltration, as well as elastic fiber disruption (Verhoeff–Van Gieson staining), and increase in smooth muscle α-actin (SM α-actin) expression in RvD1-treated WT mice, but not in RvD1-treated FPR2$^{-/-}$ mice. Arrows indicate areas of immunostaining. $^{*}p < .02$; $^{\#}p < .01$ versus WT Elastase; $^{\delta}p < .01$ versus WT Elastase+RvD1; ns, not significant; $n = 5$ mice/group.

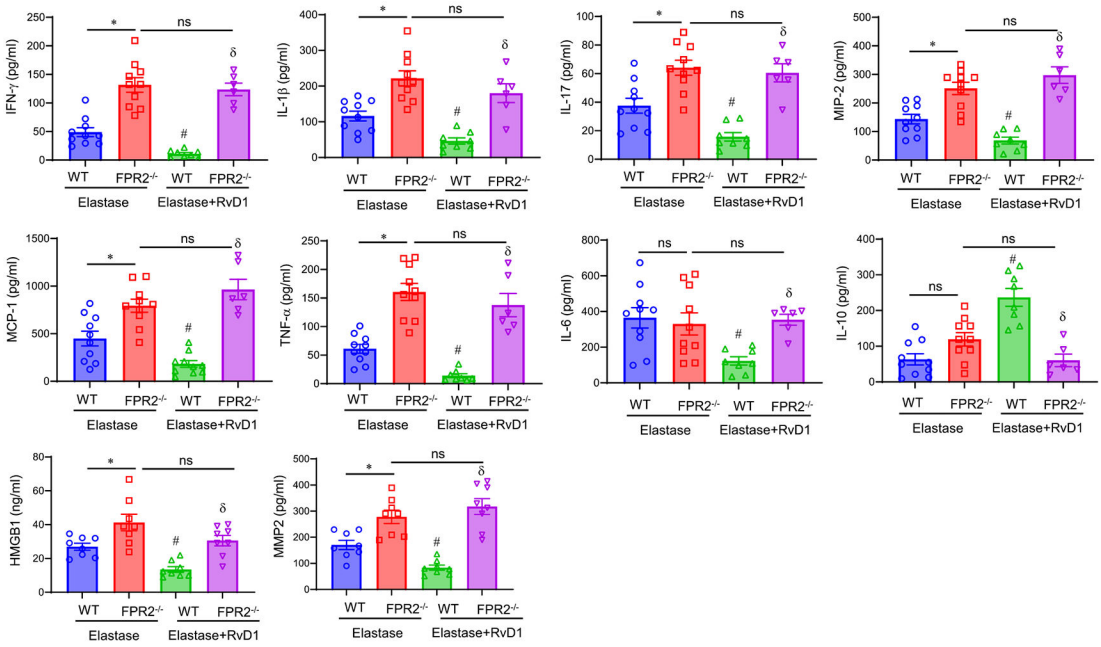

FIGURE 6.

Aortic inflammation is mitigated by RvD1/FPR2 signaling. Aortic tissue from elastase-treated WT mice after RvD1 administration showed a significant attenuation in proinflammatory cytokine/chemokine production and MMP2 expression, and a significant upregulation of IL-10 expression, compared to RvD1-treated $FPR2^{-/-}$ mice. $^{*}p < .02$; $^{\#}p < .01$ versus WT Elastase; $^{\delta}p < .001$ versus WT Elastase+RvD1; ns, not significant; $n =$ 6–10/group.

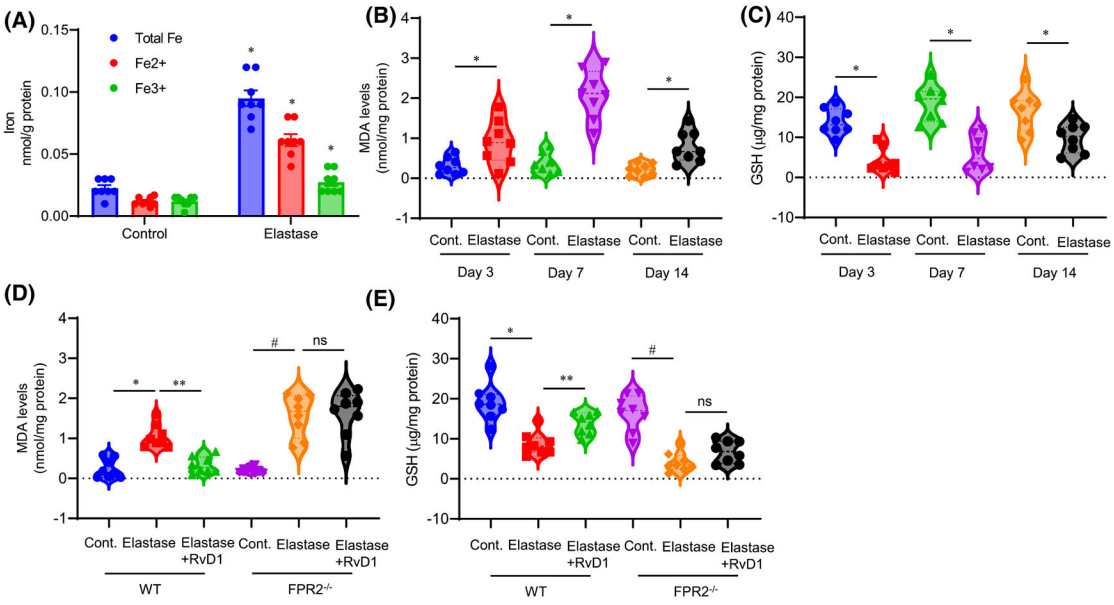

FIGURE 7.

RvD1/FPR2 signaling mitigates ferroptosis. A significant change in hallmarks of ferroptosis, that is, increase in endogenous Fe and lipid peroxidation (MDA), as well as depletion of glutathione (GSH) occurs in aortic tissue after AAA. (A) Increase in Fe and Fe^{2+} levels in aortic tissue of elastase-treated WT mice were observed compared to heat-inactivated controls on day 14. *$p < .02$ versus respective controls; $n = 8$/group. (B) A significant increase in MDA expression was observed in elastase-treated WT mice compared to respective controls on days 3, 7, and 14. *$p < .02$ versus respective controls; $n = 8$/group. (C) A significant decrease in GSH expression was observed in elastase-treated WT mice compared to respective controls on days 3, 7 and 14. *$p < .01$ versus respective controls; $n = 8$/group. (D) RvD1 treatment significantly decreased MDA expression in aortic tissue of elastase-treated WT mice, but not in $FPR2^{-/-}$ mice, on day 14. *$p < .01$ versus WT Control; **$p < .01$ versus WT Elastase; $^{\#}p < .01$ versus $FPR2^{-/-}$ Control; ns, not significant; $n = 8$/group. (E) RvD1 treatment significantly increased GSH expression in aortic tissue of elastase-treated WT mice, but not in $FPR2^{-/-}$ mice, on day 14. *$p < .01$ versus WT Control; **$p < .01$ versus WT Elastase; $^{\#}p < .01$ versus $FPR2^{-/-}$ Control; ns, not significant; $n = 8$/group.

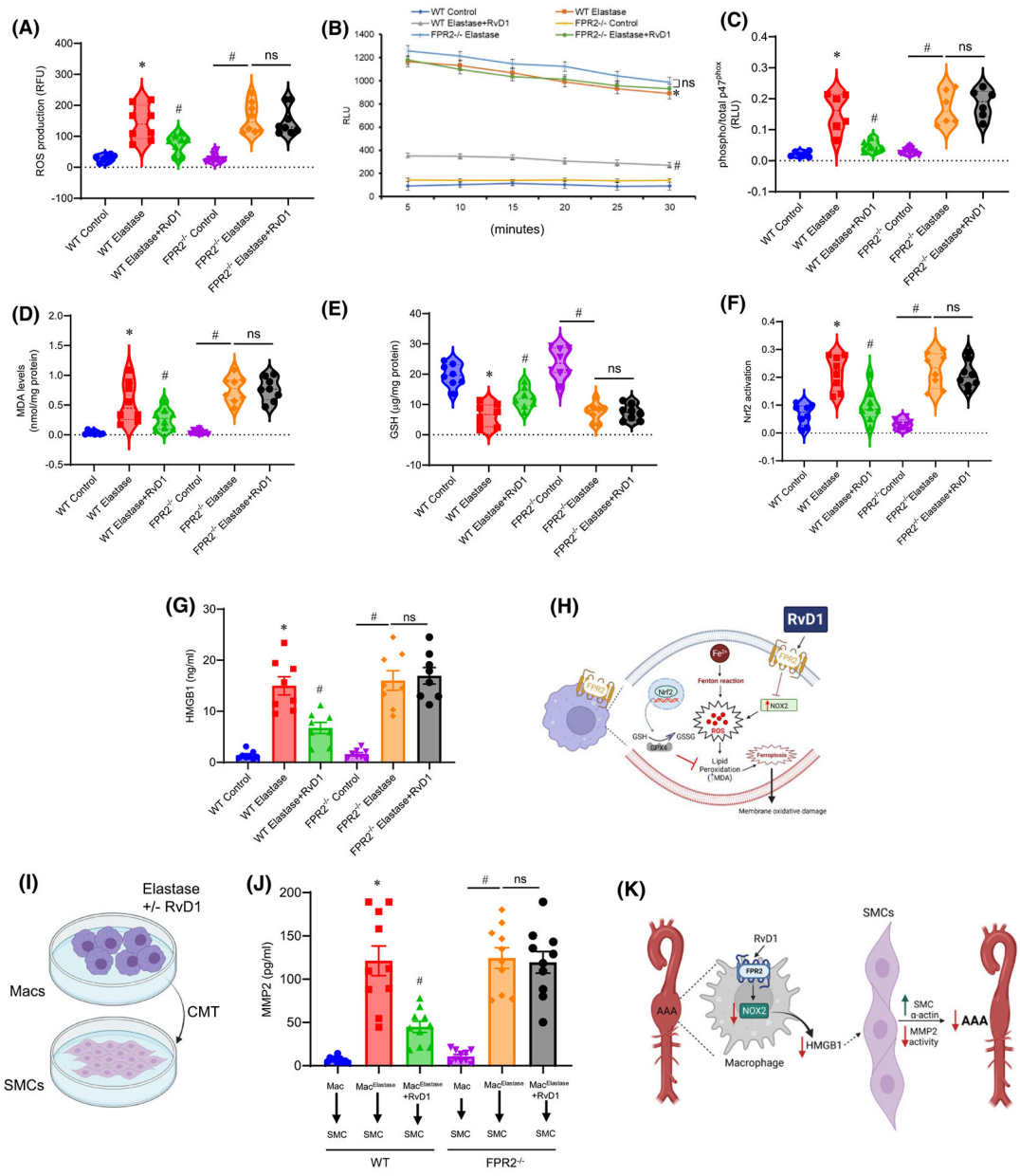

FIGURE 8.

RvD1/FPR2 signaling attenuates superoxide generation and p47^{phox} phosphorylation in macrophages to decrease ferroptosis. (A) Total reactive oxygen species (ROS) production was quantified in murine F4/80+ macrophages from WT and FPR2$^{-/-}$ mice using dichlorofluorescein dye and measuring relative fluorescence units (RFU). Transient elastase-treatment markedly increased ROS production, which was markedly reduced by RvD1 treatment in macrophages from WT mice, but not in macrophages from FPR2$^{-/-}$ mice. *p < .001 versus WT Control; $^{\#}p$ < .01 versus WT Elastase; $^{\#}p$ < .01 versus FPR2$^{-/-}$ Control; ns, not significant; relative fluorescence units (RFUs). (B) Elastase-exposed macrophages displayed significant superoxide anion generation compared with controls, which was significantly attenuated by RvD1 treatment in macrophages from WT mice, but not in

macrophages from FPR2$^{-/-}$ mice. *$p < .0001$ versus WT Control; $^{\#}p < .001$ versus WT Elastase; ns, not significant; $n = 8$/group; relative light units (RLUs). (C) Phosphorylation of p47^{phox} (ratio of phosphorylated to total p47^{phox} in RLU) in macrophages was significantly elevated after elastase treatment, which was blocked by RvD1 treatment in macrophages from WT mice, but not in macrophages from FPR2$^{-/-}$ mice. *$p < .0001$ versus WT Control; $^{\#}p < .001$ versus WT Elastase; $^{\#}p < .01$ versus FPR2$^{-/-}$ Control; ns, not significant; $n = 8$/group. (D) A significant increase in MDA expression is cell culture extracts was observed in elastase-treated macrophages which was abolished by RvD1 treatment in WT macrophages but not in FPR2$^{-/-}$ macrophages. *$p < .0001$ versus WT Control; $^{\#}p < .001$ versus WT Elastase; $^{\#}p < .01$ versus FPR2$^{-/-}$ Control; ns, not significant; $n = 8$/group. (E) A significant decrease in glutathione levels was observed in elastase-treated macrophages which was significantly attenuated by RvD1-treatment in macrophages from WT mice, but not in macrophages from FPR2$^{-/-}$ mice. *$p < .001$ versus WT Control; $^{\#}p < .001$ versus WT Elastase; $^{\#}p < .01$ versus FPR2$^{-/-}$ Control; ns, not significant; $n = 8$/group. (F) Nuclear translocation of Nrf2 was significantly increased in elastase-treated macrophages which was significantly attenuated by RvD1-treatment in macrophages from WT mice, but not in macrophages from FPR2$^{-/-}$ mice. *$p < .001$ versus WT Control; $^{\#}p < .001$ versus WT Elastase; $^{\#}p < .01$ versus FPR2$^{-/-}$ control; ns, not significant; $n = 8$/group. (G) Measurement of HMGB1 expression from macrophage cultures demonstrated a multi-fold increase after elastase treatment which was mitigated by RvD1 treatment in WT macrophages but not in FPR2$^{-/-}$ macrophages. *$p < .0001$ versus WT Control; $^{\#}p < .01$ versus WT Elastase; $^{\#}p < .01$ versus FPR2$^{-/-}$ Control; ns, not significant; $n = 8$/group. (H) Schematic description of RvD1/FPR2-mediated signaling in macrophages demonstrating inactivation of phosphorylated p47^{phox} subunit of Nox2 which decreases ROS production and lipid peroxidation, leading to restoration of glutathione levels and impediment of Nrf2 nuclear translocation. Prevention of Nox2-mediated ROS and ferroptosis decreases by RvD1/FPR2 leads to decrease in HMGB1 secretion (I and J) Conditioned media transfer (CMT) from elastase-exposed macrophages to smooth muscle cells (SMCs) induced a significant increase in MMP2 expression, which was attenuated by RvD1 treatment of macrophages from WT mice, but not in FPR2$^{-/-}$ macrophages. *$p < .0001$ versus WT Control; $^{\#}p < .01$ versus WT Elastase; $^{\#}p < .01$ versus FPR2$^{-/-}$ Control; ns, not significant; $n = 8$/group. (K) Schematic representation of signaling events during the crosstalk between macrophages and SMCs to modulate AAA formation. RvD1/FPR2 signaling prevents Nox2 activation and HMGB1 secretion by macrophages, thereby decreasing SMC activation and inhibition of MMP2 activity. This collective decrease in aortic inflammation and vascular remodeling leads to decrease in AAA formation. RvD1, Resolvin D1; Nox2, NADPH oxidase 2, SMC, smooth muscle cells; Macs, macrophages; Nrf2, nuclear factor erythroid 2-related factor 2.